192

Isomorphic multifractal shear flows for hard disks via adiabatic and isokinetic nonequilibrium molecular dynamics

Christoph Dellago

Department of Chemistry, University of California at Berkeley, Berkeley, California 94720

Wm. G. Hoover

Department of Applied Science, University of California at Davis–Livermore and Lawrence Livermore National Laboratory, Livermore, California 94551-7808

Harald A. Posch

Institute for Experimental Physics, University of Vienna, Boltzmanngasse 5, Wien A-1090, Austria

Identical particle trajectories can result from driven shear flows of two different types: (i) thermostatted flows, simulating a nonequilibrium steady state, and (ii) adiabatic flows, in which the irreversible heating associated with viscous work is not extracted from the system. This trajectory isomorphism applies to shears of hard particles, such as hard disks and spheres. Here we simulate such isomorphic shear flows. We also discuss the associated instantaneous Lyapunov spectra, which are not isomorphic. We extrapolate the dissipative hard-disk spectra to the large-system limit. [S1063-651X(98)00605-9]

I. INTRODUCTION

About ten years ago it was established that reversibly thermostated nonequilibrium steady states lead to multifractal phase-space structures [1–6]. The fractal structures have "Kaplan-Yorke" or "information" phase-space dimensionalities [7,8] less than that of their equilibrium counterparts. This finding of reduced dimensionality demonstrated the rarity of nonequilibrium phase-space states relative to equilibrium ones, and explained it in terms of their singular fractal nature. The fractal distributions of nonequilibrium phase-space states are confined to "strange attractors," objects with zero measure, relative to the smooth Gibbsian equilibrium distributions. Surprisingly, the time-reversible mechanics underlying the nonequilibrium flows turned out to be perfectly consistent with dissipative singular attractors, and with the additional unexpected consequence that the resulting nonequilibrium phase-space distributions were singular, rather than smooth.

The singular multifractal phase-space structures provided an appealing mechanical rationale for the second law of thermodynamics [1]. But the thermostats underlying these structures raised a question [9,10]: "Do the fractals correctly represent the rarity of nonequilibrium states, or are these singular objects, of reduced dimensionality, merely artifacts of particular time-reversible thermostatting techniques?" A recent investigation of this question [11] established that the multifractal states found in thermostated hard-particle simulations [1–6,12] have precise counterparts in somewhat-more-conventional adiabatic flows. Here we study the relationships between two types of shear-flow problems, the one adiabatic and the other thermostated with a fixed kinetic energy ("isokinetic"). It is remarkable that these two very different problem types can generate configuration-space trajectories, $\{y(x)\}_N$, which are "isomorphic," meaning "having the same shape."

A nonequilibrium "time scaling," which is reminiscent of Nosé's equilibrium work [13], links the two simulation types, and also makes it possible to correlate the corresponding instantaneous dissipation rates and the phase-space distribution functions. The present work is devoted to carrying out simulations exhibiting the isomorphism property and analyzing the results. Though we find, on the one hand, that the particle trajectories are indeed isomorphic, as the analysis of Ref. [11] suggests, on the other hand we discover that the instantaneous Lyapunov spectra are not simply related to one another.

The present work is described as follows. In Sec. II we discuss isomorphisms which link together a variety of approaches to the simulation of many-body hard-particle nonequilibrium flows. In Sec. III we show that the configurational trajectory isomorphism leads to a simple scaling of the instantaneous Lyapunov sums, in the full phase space $\{x,y,p_x,p_y\}_N$. Section IV includes a brief review of shear-flow techniques, using periodic boundary conditions, and emphasizing the particular difficulties associated with scaling hard-particle collisions using these boundary conditions. Section V describes our numerical simulations of shear flows, and the results obtained from them. Section VI is devoted to our conclusions.

II. TRAJECTORY ISOMORPHISMS FOR DISKS AND SPHERES

The usual Newtonian trajectories traced out by hard disks or hard spheres have shapes independent of the kinetic temperature. Quadrupling the temperature, by doubling all the particle velocities $(kT \propto \langle mv^2 \rangle)$, simply doubles the rate at which the $\{x,y\}_N$ or $\{x,y,z\}_N$ paths are traced out. The increased speed does not change the shapes of the configurational trajectories themselves. Very similar relations hold also for trajectories generated by inverse-power "soft-
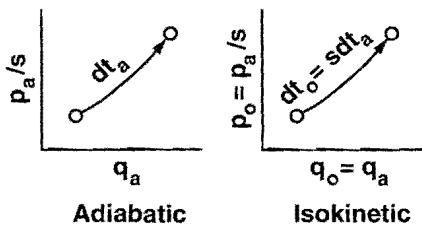
FIG. 1. Corresponding changes in isokinetic and adiabatic trajectories for a time interval $dt_0 = s\,dt_a$. The $\{y(x)\}$ representations of the trajectories are identical, though both the momenta and other rates differ, by the scale factor $s = (K_a/K_0)^{1/2}$, as is explained in the main text.

sphere'' potentials, $\phi \propto r^{-n}$, but with the added complexity that the volume and the temperature must change simultaneously [14], in a correlated way, to maintain an isomorphism. For simplicity, we specialize our numerical work to the two-dimensional hard-disk case, for which the particle trajectories are correlated sets of two-dimensional coordinates, $\{y(x)\}_N$. Exactly similar considerations follow for hard spheres.

Driven nonequilibrium simulations most often incorporate isokinetic or isoenergetic feedback forces, so as to maintain stationary states [15,16]. Though thermostat forces can be applied to a special set of boundary particles, the thermostat forces are usually applied homogeneously, to all the particles, so as to minimize the influence of the boundaries. Mass or energy currents are driven by external fields, sensitive to a particle's type or energy, while homogeneous ''shear flows'' are usually driven by special periodic shearing boundary conditions. These shearing boundary conditions were developed, independently, by at least three separate sets of workers [17–19]. The shearing boundaries preclude the conservation of total energy, or internal energy, or angular momentum, whether or not thermostating feedback forces are present.

The idea underlying a trajectory isomorphism between adiabatic and isokinetic thermostated trajectories can be visualized as indicated in Fig. 1, where the progress of two isomorphic trajectories, but in two different phase spaces, is outlined schematically. In the figure, we show the correspondence between trajectories in (i) the adiabatic phase space $\{q_a, p_a\}_N$ and in (ii) the isokinetic phase space $\{q_0, p_0\}_N$. Notice that, while the trajectories agree exactly, the momenta differ by a scale factor s, discussed below. We indicate variables following the two types of trajectories by subscripts a for adiabatic and 0 for isokinetic. The isomorphism linking the two trajectory types implies that all the geometric configurational variables, based on particle coordinates, are identical in the two corresponding trajectory segments:

$$(x,y)_a \Leftrightarrow (x,y)_0.$$

On the other hand, rates, such as the particle velocities and the strain rate—defined more fully in Sec. IV, are different, and typically become faster in the adiabatic flow, as the kinetic energy of that flow increases due to viscous heating:

$$(1/dt, \dot{x}, \dot{y}, p_x, p_y, \dot{\epsilon})_a \Leftrightarrow s(1/dt, \dot{x}, \dot{y}, p_x, p_y, \dot{\epsilon})_0,$$

$$s \equiv (K_a/K_0)^{1/2} \equiv dt_0/dt_a.$$

Here, and throughout this work, we represent, by s, the ''scale factor'' which correlates the isokinetic and adiabatic time scales. The treatment of second derivatives, including the accelerations and the dissipation rate, discussed in the following section, is somewhat more complicated. For the accelerations, a chain-rule calculation establishes the useful correspondence

$$(\dot{p})_a = s(d/dt)_a(sp_0) \Leftrightarrow s^2[\dot{p} + (\dot{K}_a/2K_a)p]_0 \equiv s^2[\dot{p} + \zeta_K p]_0,$$

where

$$(\dot{s}/s)_a \equiv \dot{K}_a/2K_a \equiv \zeta_K.$$

Thus the isokinetic friction coefficient ζ_K, described in more detail, for shear flows, in Sec. IV, corresponds to the rate of change of the thermal energy along the corresponding adiabatic trajectory.

An analytic demonstration of the trajectory isomorphism [11] can be based on showing that the trajectory curvatures $\{d^2y/dx^2\}_N$ match, at corresponding trajectory points $\{x,y\}_N$ with matching slopes, $\{dy/dx = p_y/p_x\}_N$. The trajectory isomorphism is most easily grasped and appreciated by comparing numerical solutions of the two sets of equations. Provided that the initial conditions correspond, exactly the same $\{y(x)\}_N$ trajectories are traced out, but at different rates. Similar scalings have been considered by several groups interested in molecular dynamics, beginning with Nosé [11,13,20–22].

A two-body trajectory segment illustrating shear-flow isomorphism as described by Doll's-tensor dynamics, appears in the Appendix. It is perhaps less obvious, but also true, that a corresponding exact scaling relationship connects the dissipation, through the instantaneous sum of the ''local'' Lyapunov exponents. Such a scaling does not occur for the individual exponents. Dissipation and the Lyapunov spectra are discussed in the following section.

III. DISSIPATION AND THE INSTANTANEOUS LYAPUNOV SPECTRA

The stability of stationary phase-space flows can be described by the Lyapunov spectrum $\{\lambda\}$, where the (time-averaged) exponents are numbered in descending order, with $\lambda_i \geq \lambda_{i+1}$. The individual exponents can be precisely determined as time averages [23], with an accuracy of a few parts per 1000. The largest exponent, λ_1, represents the average rate at which two nearby trajectories diverge from one another. The rate at which a two-dimensional phase-space area, defined by three neighboring trajectories, changes with time defines the sum $\lambda_1 + \lambda_2 = \langle d \ln A/dt \rangle$. Likewise, the averaged time rate of change of a three-dimensional phase-space volume, $\langle d \ln V/dt \rangle$, is equal to the sum of the largest three exponents, $\lambda_1 + \lambda_2 + \lambda_3$. The technical details underlying the computation of the spectrum have been comprehensively described for hard disks and spheres [23,24].

The Lyapunov exponents provide an important link between microscopic mechanics and macroscopic irreversible thermodynamics. Their instantaneous sum provides a direct measure of dissipation, through the external entropy production $\dot{S}$ [15,16]:

$$\dot{S}/k = -\sum \lambda_i ,$$

with the sum including all the Lyapunov exponents. Thus external entropy production corresponds to the time-averaged rate at which the comoving phase-space volume—$4N$ dimensional for N hard disks and $6N$ dimensional for N hard spheres—decreases. Evidently the occupied phase volume characterizing a stationary state can neither increase nor decrease. Thus the dimensionality of a steady-state phase-space attractor is equal to the linearly interpolated number of terms in the partial sum $\sum' \lambda_i$ at which the interpolated sum [7] changes from positive (indicating growth) to negative (indicating decay). This borderline dimensionality is generally fractional. It is the "information dimension" or "Kaplan-Yorke dimension," of the strange attractor, to which the dynamics of the stationary state distribution is effectively confined.

In the full phase space, both the adiabatic and the isokinetic dynamics must satisfy the phase-space continuity equation [15,16,25]:

$$d \ln f/dt \equiv -\sum \lambda_i = -\sum (\partial \dot{q}/\partial q) - \sum (\partial \dot{p}/\partial p),$$

despite the fact that both dynamics inhabit multifractals with an information dimension well below that of the full space. Taking into account that Gibbs's canonical hard-disk equilibrium phase-space distribution f_{eq} varies as $(VT)^{-N}$, gives an interesting and useful relation linking the evolving nonequilibrium phase-space density to the corresponding equilibrium phase-space distribution:

$$d \ln(f_{neq}/f_{eq})/dt = -\sum (\partial \dot{q}/\partial q) - \sum (\partial \dot{p}/\partial p) + N\dot{K}_a/K_a$$

$$\equiv \Delta \dot{S}/k = -\sum \lambda_i ,$$

where ΔS is the excess entropy, relative to an ideal gas at the same energy, and the Lyapunov exponents are those of the nonequilibrium distribution. Though this relationship holds for both thermostated and adiabatic shear flows, the individual instantaneous Lyapunov exponents are not simply related to one another. The exponents are sensitive to the rates at which particle trajectories are generated as well as to the trajectory shapes.

In the following section, we consider the relations linking the dissipation to the Lyapunov spectrum, for both adiabatic and isokinetic shear flows. In the adiabatic case the phase-space density f_{neq} increases, relative to the equilibrium one, mainly due to an increase in the kinetic energy:

$$Nk\dot{T} = \eta \dot{\epsilon}^2 V .$$

There is an additional small contribution due to the momentum dependence of the scale factor s. In the isomorphic isokinetic case f_{neq} increases, mainly due to the frictional concentration of phase-space density, through the friction coefficient ζ_K. There is also a smaller contribution from the momentum derivative of ζ_K. We will see that the relative rate of increase, $\Delta \dot{S}/k = d \ln(f_{neq}/f_{eq})/dt$, is the same in both

cases. As the system size is increased, with the dissipation approaching ever more closely to the macroscopic hydrodynamic prediction, s, T, and the dissipation rate all come to follow simple analytic forms [11].

IV. SHEAR-FLOW SIMULATIONS

As is the usual practice, we consider plane Couette flow here, with the strength of the departure from equilibrium described by a homogeneous "strain rate," $\dot{\epsilon} \equiv du_x/dy$. It is also usual to use feedback constraint forces to extract the thermodynamic work done by the periodic shear. During the time interval t the work done by the shear stress $-P_{xy}$ is

$$W(t) \equiv -\int_0^t P_{xy} V \dot{\epsilon} \, dt' .$$

By applying feedback, in the form of frictional constraint, or "thermostat," forces $\{-\zeta p\}$ either the "temperature" $\propto \langle p^2/(mk) \rangle$ or the "internal energy" $E = \Phi + \sum p^2/2m$—where the "momenta" $\{p\}$ are defined relative to the local stream velocity—can be controlled. For hard disks and spheres the difference between these two approaches is of order $1/N$.

In what follows we consider isokinetic shear-flow dynamics of periodic N-body systems in two space dimensions. For simplicity we let the systematic shearing motion vary linearly in space, $u_x = \dot{\epsilon} y$. The corresponding thermostated equations of motion—with the presence of a thermostat again indicated by a subscript 0—can be written in terms of a parameter α which further distinguishes among families of shear-flow models:

$$\{\dot{x} = \dot{\epsilon} y + p_x/m; \dot{y} = p_y/m; \dot{p}_x = F_x - \alpha \dot{\epsilon} p_y - \zeta p_x; \dot{p}_y$$
$$= F_y - (1-\alpha) \dot{\epsilon} p_x - \zeta p_y\}_0 .$$

The friction coefficient ζ in these equations of motion provides the dissipation described in the preceding section. "Doll's-tensor" dynamics, which we adopt in our numerical work, corresponds to the choice $\alpha = 0$ while "sllod" [15] dynamics corresponds to the alternative $\alpha = 1$. For any α, the isokinetic and isoenergetic forms for the friction coefficient ζ are given by relatively simple functions of the particles' coordinates and momenta:

$$\zeta_K = \sum [F(p/m) - \dot{\epsilon}_0(p_x p_y/m)]/2K \approx \zeta_E = -\dot{\epsilon} P_{xy} V/2K .$$

Apart from small number-dependent corrections, these friction coefficients are also directly related to the rate of divergence of the phase-space density function f_{neq}, as was outlined in Sec. III:

$$d \ln f_{neq}/dt = 2N\zeta + O(1/N) .$$

In the adiabatic case the increase in the strain rate with time contributes ζ_K to $d \ln f_{neq}/dt$. The decreasing value of the equilibrium distribution function, $\propto T^{-N}$, provides a contribution N times larger. In the isokinetic case the correspond-

ing equilibrium distribution is stationary; the thermostatting friction forces $\{-\zeta_K p\}_N$ provide the entire increase in the phase-space density:

$$d \ln f_{\text{neq}}/dt = (2N)\zeta_K .$$

Between collisions, where the interparticle forces vanish and the shear stress is purely kinetic, the isokinetic and isoenergetic friction coefficients would be exactly the same. During the isolated two-body collisions, the two friction coefficients would differ slightly, again by terms of order $1/N$, only becoming identical as the number of particles increases. The collisional contributions make highly singular, δ-function contributions to the motion of all the particles, at the instant of each two-body collision. Although these collisional contributions can be ignored at low density, they provide most of the frictional dissipation at high density, for both shear flows and heat flow.

Apart from the friction coefficient ζ, Doll's-tensor dynamics follows from a special Hamiltonian, designed to model either shear or bulk adiabatic flows [26]:

$$\mathcal{H}_{\text{Doll}}^{qp} = \Phi(\{q\}) + K(\{p\}) + \sum \nabla u : qp .$$

In the plane Couette flows considered here, the corresponding nonequilibrium Hamiltonian $\mathcal{H}_{\text{Doll}}^{qp}$ includes the terms $\{\dot{\epsilon}y p_x\}$, one for each particle. The alternative sllod dynamics [16] follows from Newton's equations of motion, transcribed to a locally comoving frame. But because the shearing boundaries again prevent energy conservation, neither of these approaches is more truly "fundamental" than the other. The Doll's-tensor approach has the computational and conceptual advantage that it involves no explicit contributions to the motion from the "strain acceleration" $\ddot{\epsilon}$, in the event that the strain rate varies with time.

Any of the families of many-body dynamics with $0 \leq \alpha \leq 1$ describes a simulation type which provides a shear viscosity in agreement with Green-Kubo linear-response theory [15,16] at small strain rates. In the usual stationary-state simulations the strain rate is fixed, at $\dot{\epsilon}_0$, and ζ is nonzero. For hard disks the special adiabatic friction-free scaling of the motion equations, including a variable strain rate, $\dot{\epsilon}_a \equiv s\dot{\epsilon}_0$, is suggested by the equations of motion. Because both the impulsive forces $\{F\}$ and the equivalent accelerations $\{\dot{p}/m\}$ are separately proportional to the collision rate, $\propto T^{1/2}$, as well as to the velocity, again $\propto T^{1/2}$, both the forces and the accelerations are proportional to temperature. If, in addition, the strain rate were chosen to be proportional to $T^{1/2}$ then the corresponding adiabatic trajectories, with zero friction, become isomorphic to their thermostated twins:

$$\{\dot{\epsilon}_a \equiv s\dot{\epsilon}_0 ; \zeta \equiv 0\} \Rightarrow \{y(x)\}_a \equiv \{y(x)\}_0 .$$

The treatment of shear-flow collisions themselves presents a difficulty which cannot be avoided. At high density most of the transport of momentum and energy occurs through isolated δ-function collisions linking pairs of particles. Trajectory isomorphism requires that each collision must lead to the same changes in the scaled velocities:

$$\delta v_0 / K_0^{1/2} \equiv \delta v_a / K_a^{1/2} .$$

Otherwise, a rescaling of all the adiabatic disk velocities would be required whenever two disks collided. This difficulty only disappears in the large-system limit, where a nearly continuous collision frequency leads to a nearly continuous variation of the kinetic-energy ratio $s^2 = (K_a/K_0)$.

To achieve some simplicity in a practicable molecular dynamics simulation, with a few hundred particles, it is essential that the "adiabatic" hard-disk collisions follow the isokinetic collision rule. Otherwise not only the strain rate but also all the particle momenta would have to undergo artificial discontinuous changes whenever any pair of disks collided. We make this arbitrary choice in discussing thermostated simulations in terms of an adiabatic analog, in the next section.

V. NONEQUILIBRIUM HARD-DISK SHEAR SIMULATIONS

In thermostated systems of hard disks or spheres the collisions need to be treated specially [27–30]. The external shear together with the isokinetic constraint affect the time evolution of the particles during their infinitesimally short impulsive collisions. Exact collision rules can be derived [22] by using an approach proposed by Hoover and Kratky [27,28] and applied to the sheared Lorentz gas by Petravic, Isbister, and Morriss [29,30]. The main idea is to replace the hard interaction by a smooth but very steep potential. One can, for example, assume that particles repel one another with a constant force F, whenever their distance is less than the particle diameter. For $F \to \infty$ the equations of motion during a two-particle collision simplify considerably and can be solved analytically. The postcollisional momenta are then related to the precollisional momenta by a one-dimensional implicit equation, which can be easily solved numerically. Corresponding exact collision rules can be derived also for tangent-space dynamics. We note the isokinetic, isoenergetic, and adiabatic collisions differ only by terms of the order $1/N$.

We confined our simulations to a single convenient density, one-fourth the close-packed density, and to a strain rate, $\dot{\epsilon} = 0.75\sigma(m/kT)^{1/2}$, large enough for multifractal effects to be important, but without entering the "string-phase" regime, which appears at large strain rates. There is nothing specially complicated about the simulations. For convenience, we choose the particle mass m, Boltzmann's constant k, the temperature T, and the disk diameter σ all equal to unity. The shapes of the periodic systems we study are initially square.

We accumulated accurate Lyapunov spectra and measured the corresponding dissipation rates for systems ranging from $N = 2$ to $N = 196$. The largest Lyapunov exponent, the sum of all the positive isokinetic exponents, and the loss of phase-space dimensionality ΔD, are all given in Table I, along with the mean dissipation rate $\langle \zeta \rangle = \langle \dot{S}/2Nk \rangle$, and the fluctuation of its kinetic part. Additional studies of the largest Lyapunov exponent λ_1, not included in Table I, established, first, that the number-dependent part of that exponent is accurately proportional to $N^{-1/2}$, and second, that convergence of the full spectrum of exponents (which requires the

TABLE I. The largest Lyapunov exponent, λ_1, the sum of the positive Lyapunov exponents, $\Sigma\lambda_+$, and the dimensionality loss per phase-space dimension, $\Delta D/(4N+1)$, are given, followed by the time-averaged values of the friction coefficient ζ and the fluctuations of the streaming contributions of ζ. All the data are for N hard disks at a density equal to one-fourth the close-packed density, and a reduced strain rate of 0.75.

N	λ_1	$\Sigma\lambda_+/N$	$\Delta D/(4N+1)$	$\langle\zeta\rangle$	$N\langle(\delta\zeta)^2\rangle$
2	2.78	1.39	0.037	0.298	0.258
4	2.10	1.70	0.051	0.275	0.178
9	2.06	1.83	0.058	0.265	0.118
16	2.14	1.86	0.061	0.270	0.123
36	2.25	1.87	0.062	0.271	0.123
64	2.31	1.87	0.062	0.270	0.122
100	2.35	1.87	0.063	0.272	0.123
144	2.38	1.87	0.062	0.271	0.124
196	2.38	1.87	0.062	0.270	0.122

solution of $4N+2$ sets of $4N+1$ coupled differential equations for N hard disks) is not currently practical beyond $N=196$. The extrapolated spectrum for $N=\infty$, based on an $N^{-1/2}$ extrapolation, is shown in Fig. 2. The gap between the positive and negative branches of the spectrum is noteworthy.

In view of our finding that the nonequilibrium fluctuations behave well, as $N^{-1/2}$ in the large-system limit, we expect the N-body dynamics to approach a well-defined large-system limit corresponding to a constant friction coefficient ζ. When fluctuations in the isokinetic dissipation rate can be ignored, so that $\zeta\equiv\zeta_0$ is constant, the relationship between the adiabatic and isokinetic time scales becomes simple:

$$d\ \ln s/dt_0=\zeta_0\rightarrow s=e^{\zeta_0 t_0}, dt_0/dt_a\equiv s=e^{\zeta_0 t_0}\rightarrow t_a$$

$$=[1-e^{-\zeta t_0}]/\zeta.$$

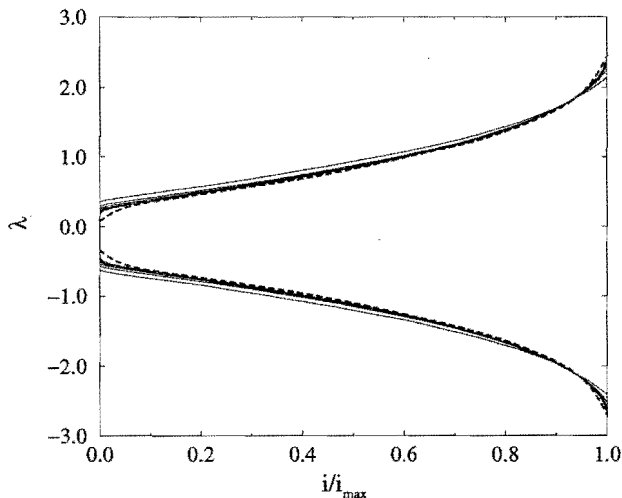An amusing consequence of this relationship linking the adiabatic and isokinetic time scales is that the infinitely long

FIG. 2. Lyapunov spectra for $N=16,36,64,100,144,196$. The vanishing exponents and the corresponding negative exponents have been omitted. Lyapunov spectra for systems of 100 and 196 hard disks are used to extrapolate to the large-system limit based on a number dependence of order $N^{-1/2}$. The dashed line indicates this extrapolated ''hydrodynamic limit'' spectrum.

isokinetic trajectories correspond to only a finite time in the adiabatic case. Nonetheless, the adiabatic trajectories include an infinite number of collisions. In fact, the effect of finite-system fluctuations on this scaling relation limits its usefulness to finite times, of the order of $\ln N$. This painfully slow convergence to the large-system limit is characteristic of fractal phase-space distributions.

VI. CONCLUSIONS

We have successfully characterized hard-disk shear flows which exhibit a detailed trajectory isomorphism linking thermostated and adiabatic flows. The fractal phase-space structures already known to be generated by thermostated simulations describe also their adiabatic analogs. We found that the individual instantaneous Lyapunov exponents for the two flow types are not simply related to each other. The summed spectra do satisfy a simple scaling rule, $\Delta\dot{S}/k=-\Sigma\lambda_i$, where ΔS is Gibbs's entropy, relative to that of an ideal gas with the same internal energy and at the same density. The number dependence of our simulation results confirmed our expectation, based on the central limit theorem, that the effect of fluctuations on intensive properties would decrease as $N^{-1/2}$. For thermostatted systems this finding suggests that the large-system instantaneous dissipation rate, as well as the other hydrodynamic state variables, approach those of a system with a constant friction coefficient, as $N\rightarrow\infty$. Provided that this is true, fluctuations can be ignored and the time-scaling relationship can be simplified, as shown in the preceding section:

$$[N=\infty]\Rightarrow\ t_a\equiv[1-e^{-\zeta_0 t_0}]/\zeta_0,$$

where the friction coefficient ζ_0 corresponds to the total dissipation, including collisional contributions. The multifractal nature of the isokinetic distribution applies also to that of the instantaneous adiabatic phase-space distribution function. Thus the present work strongly suggests that the fractal structure of large-system thermostated flows also represents the limiting structure of adiabatic shear flows.

In the present work the friction coefficient linking the two types of trajectories incorporates only the streaming contributions to the shear stress. We expect that exactly similar considerations would apply as the system size is increased,

so that fluctuations in the rate of phase-space collapse (in the thermostated case) and equilibrium phase-space growth (in the adiabatic case) can likewise be ignored.

ACKNOWLEDGMENTS

APPENDIX

We demonstrate numerically the trajectory isomorphism discussed in the text, for a symmetric pair of hard disks undergoing shear according to Doll's-tensor dynamics. The motion equations are as follows:

$$\{\dot{x} = \dot{\epsilon}y + p_x/m ; \dot{y} = p_y/m ;$$

$$\dot{p}_x = F_x - \zeta p_x ; \dot{p}_y = F_y - \dot{\epsilon}p_x - \zeta p_y\},$$

where the isokinetic friction coefficient is a ratio of two-particle sums:

$$\zeta \equiv -\dot{\epsilon}\sum p_x p_y \bigg/ \sum p^2.$$

The adiabatic equations are exactly similar except that the strain rate $\dot{\epsilon}$ varies with the kinetic energy:
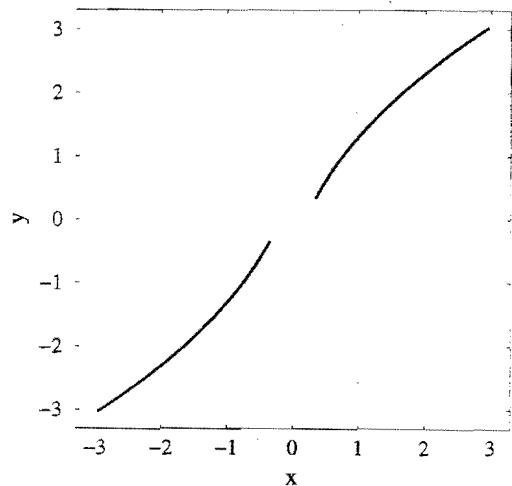

FIG. 3. A pair of time-reversible hard-disk trajectories $\{y(x)\}$ according to both isokinetic—constant-strain-rate—dynamics and adiabatic—scaled-strain-rate—dynamics, as is described in the Appendix.

$$\dot{\epsilon}(t) \equiv s\dot{\epsilon}(0), s \equiv [K(t)/K(0)]^{1/2}.$$

The forces $\{F_x, F_y\}$ represent the hard-particle collisions. We display a simple numerical example in Fig. 3. The initial "momenta" of the two disks, which describe their motion relative to the local stream velocity, are taken to be $\{\pm 5/13, \pm 12/13\}$, so that the initial comoving kinetic energy is unity. The strain rate is $0.25\sigma(m/kT)^{1/2}$, one-third that used in our many-body simulations. The trajectories shown in Fig. 3 correspond to an isothermal time interval of 3.0000 and to an adiabatic time interval of 3.4762. Both sets of motion equations yield the same laboratory-frame trajectories, as shown here.

[1] B. L. Holian, W. G. Hoover, and H. A. Posch, Phys. Rev. Lett. **59**, 10 (1987).

[2] W. G. Hoover, H. A. Posch, B. L. Holian, M. J. Gillan, M. Mareschal, and C. Massobrio, Mol. Simul. **1**, 79 (1987).

[3] B. Moran, W. G. Hoover, and S. Bestiale, J. Stat. Phys. **48**, 709 (1987).

[4] G. Morriss, Phys. Lett. A **122**, 236 (1987).

[5] W. G. Hoover, B. Moran, B. Holian, H. Posch, and S. Bestiale, in *Shockwaves in Condensed Matter 1987*, edited by S. C. Schmidt and N. C. Holmes (North-Holland, Amsterdam, 1988).

[6] W. G. Hoover, Phys. Rev. A **37**, 252 (1988).

[7] J. L. Kaplan and J. A. Yorke, in *Functional Differential Equations and Approximations of Fixed Points*, edited by H. O. Peitgen and H. O. Walther (Springer-Verlag, Berlin, 1979).

[8] J. D. Farmer, E. Ott, and J. A. Yorke, Physica D **7**, 153 (1983).

[9] See the discussions in *Microscopic Simulations of Complex Hydrodynamic Phenomena*, Vol. 292 of *NATO Advanced Study Institute, Series B: Physics*, edited by M. Mareschal and B. L. Holian (Plenum, New York, 1992).

[10] M. Mareschal, in *Advances in Chemical Physics*, edited by I.

Prigogine and S. A. Rice (Wiley, New York, 1997), Vol. 100, p. 317.

[11] Wm. G. Hoover, Phys. Lett. A **235**, 357 (1997).

[12] N. I. Chernov, G. L. Eyink, J. L. Lebowitz, and Y. G. Sinai, Phys. Rev. Lett. **70**, 2209 (1993).

[13] S. Nosé, Prog. Theor. Phys. Suppl. **103**, 1 (1991).

[14] W. G. Hoover, S. G. Gray, and K. W. Johnson, J. Chem. Phys. **55**, 1128 (1971).

[15] W. G. Hoover, *Computational Statistical Mechanics* (Elsevier, Amsterdam, 1991).

[16] D. J. Evans and G. P. Morriss, *Statistical Mechanics of Nonequilibrium Liquids* (Academic Press, New York, 1990).

[17] A. W. Lees and S. F. Edwards, J. Phys. C **5**, 1921 (1972).

[18] T. Naitoh and S. Ono, Phys. Lett. **57A**, 448 (1976).

[19] W. T. Ashurst, Ph.D. dissertation, University of California at Davis–Livermore, 1974.

[20] W. G. Hoover, B. Moran, C. G. Hoover, and W. J. Evans, Phys. Lett. A **133**, 114 (1988).

[21] C. P. Dettmann and G. P. Morriss, Phys. Rev. E **54**, 2495 (1996).

[22] C. P. Dettmann and G. P. Morriss, Phys. Rev. E **55**, 3693 (1997).

[23] Ch. Dellago, H. A. Posch, and W. G. Hoover, Phys. Rev. E **53**, 1485 (1996).

[24] Ch. Dellago and H. A. Posch (unpublished).

[25] Wm. G. Hoover, D. J. Evans, H. A. Posch, B. L. Holian, and G. P. Morriss, Phys. Rev. Lett. (to be published).

[26] W. G. Hoover, in *Systems Far From Equilibrium*, edited by J. Ehlers, K. Hepp, R. Kippenhahn, H. A. Weidenmüller, and J. Zittartz, Lecture Notes in Physics Vol. 132 (Springer, Berlin, 1980), p. 373.

[27] W. G. Hoover and K. W. Kratky, J. Stat. Phys. **42**, 1103 (1986).

[28] K. W. Kratky and W. G. Hoover, J. Stat. Phys. **48**, 873 (1987).

[29] J. Petravic and D. J. Isbister, Phys. Rev. E **51**, 4309 (1995).

[30] J. Petravic, D. J. Isbister, and G. P. Morriss, J. Stat. Phys. **76**, 1045 (1994).